JOURNAL OF THE AMERICAN COLLEGE OF CARDIOLOGY
© 2016 BY THE AMERICAN COLLEGE OF CARDIOLOGY FOUNDATION
PUBLISHED BY ELSEVIER

VOL. 67, NO. 5, 2016
ISSN 0735-1097/$36.00
http://dx.doi.org/10.1016/j.jacc.2015.10.093

Biallelic Truncating Mutations in *ALPK3* Cause Severe Pediatric Cardiomyopathy

Rowida Almomani, PhD,[a] Judith M.A. Verhagen, MD,[b] Johanna C. Herkert, MD,[a] Erwin Brosens, PhD,[b] Karin Y. van Spaendonck-Zwarts, MD, PhD,[a,c] Angeliki Asimaki, PhD,[d] Paul A. van der Zwaag, MD, PhD,[a] Ingrid M.E. Frohn-Mulder, MD,[e] Aida M. Bertoli-Avella, MD, PhD,[b,f] Ludolf G. Boven, BSc,[a] Marjon A. van Slegtenhorst, PhD,[b] Jasper J. van der Smagt, MD,[g] Wilfred F.J. van IJcken, PhD,[h] Bert Timmer, MD, PhD,[i] Margriet van Stuijvenberg, MD, PhD,[j] Rob M. Verdijk, MD, PhD,[k] Jeffrey E. Saffitz, MD, PhD,[d] Frederik A. du Plessis, MD,[e] Michelle Michels, MD, PhD,[l] Robert M.W. Hofstra, PhD,[b] Richard J. Sinke, PhD,[a] J. Peter van Tintelen, MD, PhD,[a,c,m] Marja W. Wessels, MD, PhD,[b] Jan D.H. Jongbloed, PhD,[a] Ingrid M.B.H. van de Laar, MD, PhD[b]

ABSTRACT

BACKGROUND Cardiomyopathies are usually inherited and predominantly affect adults, but they can also present in childhood. Although our understanding of the molecular basis of pediatric cardiomyopathy has improved, the underlying mechanism remains elusive in a substantial proportion of cases.

OBJECTIVES This study aimed to identify new genes involved in pediatric cardiomyopathy.

METHODS The authors performed homozygosity mapping and whole-exome sequencing in 2 consanguineous families with idiopathic pediatric cardiomyopathy. Sixty unrelated patients with pediatric cardiomyopathy were subsequently screened for mutations in a candidate gene. First-degree relatives were submitted to cardiac screening and cascade genetic testing. Myocardial samples from 2 patients were processed for histological and immunohistochemical studies.

RESULTS We identified 5 patients from 3 unrelated families with pediatric cardiomyopathy caused by homozygous truncating mutations in *ALPK3*, a gene encoding a nuclear kinase that plays an essential role in early differentiation of cardiomyocytes. All patients with biallelic mutations presented with severe hypertrophic and/or dilated cardiomyopathy in utero, at birth, or in early childhood. Three patients died from heart failure within the first week of life. Moreover, 2 of 10 (20%) heterozygous family members showed hypertrophic cardiomyopathy with an atypical distribution of hypertrophy. Deficiency of alpha-kinase 3 has previously been associated with features of both hypertrophic and dilated cardiomyopathy in mice. Consistent with studies in knockout mice, we provide microscopic evidence for intercalated disc remodeling.

CONCLUSIONS Biallelic truncating mutations in the newly identified gene *ALPK3* give rise to severe, early-onset cardiomyopathy in humans. Our findings highlight the importance of transcription factor pathways in the molecular mechanisms underlying human cardiomyopathies. (J Am Coll Cardiol 2016;67:515–25) © 2016 by the American College of Cardiology Foundation.

From the [a]University of Groningen, University Medical Center Groningen, Department of Genetics, Groningen, the Netherlands; [b]Department of Clinical Genetics, Erasmus University Medical Center, Rotterdam, the Netherlands; [c]Department of Clinical Genetics, Academic Medical Center, University of Amsterdam, Amsterdam, the Netherlands; [d]Department of Pathology, Harvard Medical School, Beth Israel Deaconess Medical Center, Boston, Massachusetts; [e]Department of Pediatric Cardiology, Erasmus University Medical Center, Rotterdam, the Netherlands; [f]Centogene AG, Rostock, Germany; [g]Department of Medical Genetics, University Medical Center Utrecht, Utrecht, the Netherlands; [h]Center for Biomics, Erasmus University Medical Center, Rotterdam, the Netherlands; [i]University of Groningen, University Medical Center Groningen, Department of Pathology and Medical Biology, Groningen, the Netherlands; [j]University of Groningen, University Medical Center Groningen, Division of Neonatology, Beatrix Children's Hospital, Groningen, the Netherlands; [k]Department of Pathology, Erasmus University Medical Center, Rotterdam, the Netherlands; [l]Department of Cardiology, Erasmus University Medical Center, Rotterdam, the Netherlands; and the [m]Durrer Center for Cardiogenetic Research, Utrecht, the Netherlands. This work was supported by funding from the Dutch Heart Foundation (2007B132, 2010B164, and 2014T007). The authors have reported that they have no relationships relevant to the contents of this

Listen to this manuscript's audio summary by *JACC* Editor-in-Chief Dr. Valentin Fuster.

ABBREVIATIONS AND ACRONYMS

DCM = dilated cardiomyopathy

DNA = deoxyribonucleic acid

HCM = hypertrophic cardiomyopathy

ICD = implantable cardiac-defibrillator

IVS = interventricular septum

LV = left ventricular

LVPW = left ventricular posterior wall

PCR = polymerase chain reaction

RNA = ribonucleic acid

RV = right ventricular

Cardiomyopathies represent a clinically and genetically heterogeneous group of disorders affecting the ventricular myocardium. Among children <18 years of age, overall incidence of cardiomyopathy is 1.13 cases per 100,000 annually in the United States (1). Pediatric cardiomyopathy is associated with significant morbidity and mortality: up to 40% of affected children die or undergo cardiac transplantation within 5 years of diagnosis (2,3). Cardiomyopathy can be classified into 5 clinical phenotypes based upon morphological and functional characteristics: hypertrophic cardiomyopathy (HCM); dilated cardiomyopathy (DCM); restrictive cardiomyopathy; arrhythmogenic right ventricular (RV) cardiomyopathy; and unclassified cardiomyopathy, including left ventricular (LV) noncompaction (4). Extremely diverse, particularly in the pediatric population, the etiology of cardiomyopathy encompasses both nongenetic and genetic causes, including myocarditis, neuromuscular diseases, inborn errors of metabolism, malformation syndromes, and familial forms caused by mutations in genes encoding the specialized, often structural, components of cardiomyocytes. Because of the routine incorporation of genetic testing in the diagnostic evaluation of patients with cardiomyopathy, a causal diagnosis can be identified in more than 70% of children (5). Interestingly, the same genetic causes that result in cardiomyopathy in adults are prevalent in the pediatric population (e.g., sarcomeric or cytoskeletal gene mutations) (6).

SEE PAGE 526

Despite recent advances in understanding the genetic etiologies of pediatric cardiomyopathy, a substantial number of cases remain unsolved, suggesting that other genes await discovery. Establishing an underlying genetic cause for cardiomyopathy allows pre-symptomatic identification of family members at risk and facilitates reproductive decision making. Genetic and genomic studies continue to provide new insights into the pathophysiological processes contributing to cardiomyopathy and will ultimately facilitate development of patient-specific prevention and treatment strategies.

To identify new genes contributing to pediatric cardiomyopathy, we used a combined approach of homozygosity mapping and whole-exome sequencing.

METHODS

We studied 4 individuals with pediatric cardiomyopathy from 2 consanguineous families of Dutch and Moroccan descent, respectively (**Figures 1A and 1B**). A third family of Turkish descent was identified by subsequent cohort screening (**Figure 1C**). Patients underwent extensive clinical investigations including high-resolution prenatal ultrasound, physical examination, 12-lead electrocardiography, transthoracic echocardiography, and post-mortem examination. Mutation screening of up to 48 known cardiomyopathy-related genes per individual was negative. A complete overview of the genetic and metabolic tests performed before this study is provided in the Online Appendix. All asymptomatic siblings and parents underwent echocardiographic screening. HCM was defined by the presence of increased LV wall thickness (>2 SD above the mean for body surface area in children or ≥13 mm in adult relatives) in the absence of hemodynamic stresses sufficient to account for the degree of hypertrophy. DCM was defined by the presence of LV dilation (LV end-diastolic dimension >2 SD above the mean for body surface area) and systolic dysfunction (fractional shortening or LV ejection fraction >2 SD below the mean for age) in the absence of abnormal loading conditions sufficient to cause global systolic impairment (4). A cohort of 60 unrelated patients with idiopathic pediatric cardiomyopathy from diverse ethnic backgrounds was available for mutational screening of candidate genes. These patients had previously been screened for mutations in 8 to 55 known cardiomyopathy-related genes. The medical ethical committees of the University Medical Center Groningen and the Erasmus University Medical Center approved this study. Written informed consent was obtained from all participants or their legal guardians.

HOMOZYGOSITY MAPPING. Genomic deoxyribonucleic acid (DNA) was extracted from peripheral blood samples (A-VIII:1, VIII:2, IX:1, and IX:2; B-III:1, IV:3, and IV:4), buccal swabs (A-IX:3 and IX:4), amniotic fluid (B-IV:1), or fibroblasts (B-IV:2) (**Figure 1**). Genome-wide

paper to disclose. Drs. Almomani and Verhagen contributed equally to this work. Drs. Jongbloed and van de Laar are joint senior authors.

Manuscript received September 8, 2015; revised manuscript received October 25, 2015, accepted October 27, 2015.

FIGURE 1 ***ALPK3*-Related Cardiomyopathy**

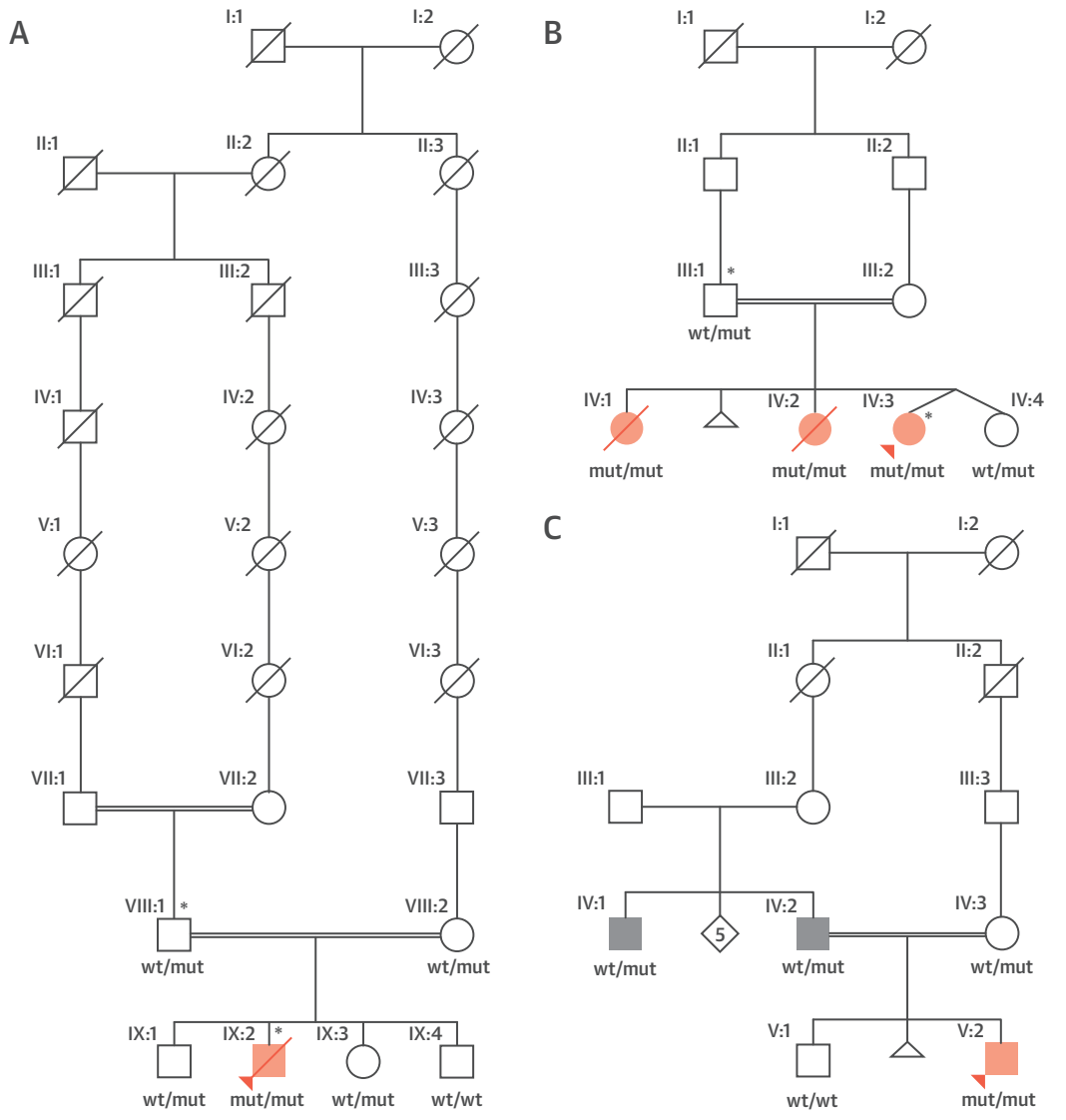

Pedigrees of families **(A, B, and C)** with alpha-kinase 3 (*ALPK3*) genetic mutations leading to cardiomyopathies. **Asterisks** = analyzed by exome sequencing; **squares** = males; **circles** = females; **solid symbols** = severely affected individuals with homozygous mutations; **gray symbols** = heterozygous individuals with adult-onset disease; **open symbols** = unaffected individuals; **diagonal lines** = deceased; **arrowheads** = index patients. *ALPK3* genotypes: mut = mutant allele; wt = wild-type allele.

genotyping was performed using the Human610-Quad BeadChip (family A) or HumanCytoSNP-12 v2.1 BeadChip (family B) array with raw data normalized and converted into genotypes using GenomeStudio data analysis software (Illumina, San Diego, California). Genotype files were uploaded into the web-based tool HomozygosityMapper to detect homozygous stretches (>5 Mb) in patients that were not present in their unaffected relatives (7).

WHOLE-EXOME SEQUENCING. Genomic DNA was sheared by sonication, then the size distribution of the fragmented DNA was analyzed, targets were captured, and paired-end sequencing (2 × 101 bp) performed. The sequence reads were mapped and aligned against the human reference genome GRCh37/hg19 (Online Appendix). Variant calling was performed, and variants were filtered on quality (read depth ≥6) and location (within an exon or

first/last 20 bp of introns). Variants with a minor allele frequency ≥1% in at least 200 chromosomes in dbSNP, the Genome of the Netherlands (8), the 1000 Genomes Project (9), or an in-house reference set, or a minor allele frequency ≥3% in the National Heart, Lung, and Blood Institute's Go Exome Sequencing Project were excluded from further analysis. Assuming an autosomal recessive model of inheritance, we selected variants found in the heterozygous state in the father and in the homozygous state in the patient. Only variants predicted to change the protein sequence (nonsynonymous single nucleotide variants and short insertions and deletions) or the recognition of consensus ribonucleic acid (RNA) splice sites were considered. Finally, we filtered for variants present in the homozygous regions.

SANGER SEQUENCING. Bidirectional Sanger sequencing of the entire coding region and exon-intron boundaries of the alpha-kinase 3 gene (*ALPK3*) was performed using polymerase chain reaction (PCR) primers (Online Table 1). PCR amplification was performed; PCR fragments were purified and sequenced, and then data were analyzed (Online Appendix). For annotation of DNA and protein changes, the mutation nomenclature recommendations from the Human Genome Variation Society were followed (10). Nucleotide numbering reflects complementary DNA (cDNA) numbering with +1 corresponding to the adenine (A) of the ATG translation initiation codon in the reference sequence NM_020778.4.

To assess the effect of the sequence variants identified on protein structure and function, we used prediction programs integrated in the Alamut Visual v2.6.1 software (Interactive Biosoftware, Rouen, France) (11–13). Furthermore, possible effects on splicing were predicted using various integrated algorithm tools.

REVERSE TRANSCRIPTASE PCR ANALYSIS. To investigate the effect of the splice site variant c.4736-1G>A at the RNA level, we performed reverse-transcription PCR analysis on RNA isolated from fibroblasts of the affected individual (A-IX:2) and 2 age-matched controls. Cells were cultured in Dulbecco's Modified Eagle Medium supplemented with 10% fetal bovine serum, 1% penicillin/streptomycin, 1% glucose, and 1% glutamax, in atmospheric oxygen and 5% CO_2 at 37° C. Total RNA was extracted, and reverse-transcription PCR was performed using gene-specific primers designed to amplify the exon expected to be affected by the mutation and flanking sequences (Online Figure 1). The resulting PCR products were examined by 2% agarose gel electrophoresis and subsequently subjected to Sanger sequencing.

HISTOLOGY. Paraffin-embedded or frozen cardiac tissue was available from 2 affected individuals (A-IX:2 and B-IV:2). Muscle biopsy specimens from the lateral portion of the quadriceps femoris muscle were available from another affected individual (B-IV:3) and her healthy sister (B-IV:4). Tissues from age-matched donors were used as controls. All samples were histologically examined after hematoxylin and eosin and desmin staining using standard techniques.

IMMUNOHISTOCHEMISTRY. Immunohistochemical analysis was performed on myocardial samples from individual A-IX:2 and 2 age-matched controls with no clinical or pathological evidence of heart disease, as described previously (14). In brief, glass-mounted sections of formalin-fixed, paraffin-embedded myocardium (5 μm) were deparaffinized and rehydrated before antibody retrieval. Primary antibodies included mouse monoclonal anti-plakoglobin (1:1,000 dilution), mouse monoclonal anti-plakophilin2 (2a+2b, undiluted), mouse monoclonal anti-desmoplakin (1:10 dilution), mouse monoclonal anti-pan cadherin (1:400 dilution), rabbit polyclonal anti-43 (1:400 dilution), and rabbit polyclonal anti-desmin (1:100 dilution). The slides were then incubated with indocarbocyanine-conjugated goat anti-mouse or goat anti-rabbit secondary antibodies (1:400 dilution). Immunostained preparations were analyzed by laser scanning confocal microscopy.

RESULTS

Results are summarized in **Table 1**. In family A, the second child of healthy Dutch parents was born at 35 weeks following an uneventful pregnancy (IX:2) (**Figure 1A**). At birth, he presented with respiratory insufficiency and cyanosis. Echocardiography showed severe LV dilation (LV end-diastolic dimension 23.5 mm; z-score unreliable because of massive edema) with markedly reduced contractility of both ventricles, and mitral and tricuspid regurgitation. He died due to progressive heart failure at 5 days. The parents agreed on autopsy (discussed in the Histology section later). Genealogical evaluation revealed that the parents were sixth-degree cousins. Family history was negative for sudden death or cardiomyopathies. Echocardiography revealed no abnormalities in his parents (ages 34 and 31 years), 2 brothers (ages 9 and 6 years), and sister (age 7 years).

In family B, the first pregnancy of these healthy consanguineous Moroccan parents (IV:1) (**Figure 1B**) included prenatal ultrasound examination at 33 weeks of gestation, revealing generalized hydrops fetalis and cardiomegaly with reduced contractility. The pregnancy ended in intrauterine fetal death

TABLE 1 Clinical Features of Affected Patients With *ALPK3* Mutations

Individual	Sex	Origin	Age at Diagnosis	Presenting Symptoms	Outcome	Genotype
A-IX:2	M	Dutch	At birth	Severe biventricular dilation	D. 5 days post-partum	Homozygous c.4736-1G>A, p.Val1579Glyfs*30
B-IV:1	F	Moroccan	33 weeks gestation	Generalized hydrops fetalis, cardiomegaly	D. 35 weeks gestation	Homozygous c.3781C>T, p.Arg1261*
B-IV:2	F	Moroccan	20 weeks gestation	Generalized hydrops fetalis, severe biventricular hypertrophy and dilation, severe tricuspid regurgitation	D. 2 h post-partum	Homozygous c.3781C>T, p.Arg1261*
B-IV:3	F	Moroccan	At birth	Severe concentric LV hypertrophy	Status quo (11 yrs)	Homozygous c.3781C>T, p.Arg1261*
C-IV:1	M	Turkish	29 yrs	Asymmetrical septum hypertrophy, RV hypertrophy	Status quo (45 yrs)	Heterozygous c.5294G>A, p.Trp1765*
C-IV:2	M	Turkish	27 yrs	Concentric LV hypertrophy with relative sparing of basal segments, RV hypertrophy	Status quo (43 yrs)	Heterozygous c.5294G>A, p.Trp1765*
C-V:2	M	Turkish	4 yrs	Severe concentric LV hypertrophy, RV hypertrophy	Ventricular fibrillation, ICD implantation (7 yrs)	Homozygous c.5294G>A, p.Trp1765*

ALPK3 = alpha-kinase 3 gene; D = death; F = female; ICD = implantable cardioverter-defibrillator; LV = left ventricular; M = male; RV = right ventricular.

at 35 weeks. External examination of the fetus did not show any gross abnormalities except massive skin edema. Autopsy was declined by the parents. Their second pregnancy resulted in a spontaneous abortion. During the third pregnancy, ultrasound examinations at 20 and 26 weeks of gestation showed an enlarged heart with severely reduced contractility, a thickened myocardium with spongy appearance, and severe tricuspid regurgitation (Figure 2A). At 30 weeks of gestation, severe fetal hydrops had

FIGURE 2 Cardiac Imaging in *ALPK3*-Related Cardiomyopathy

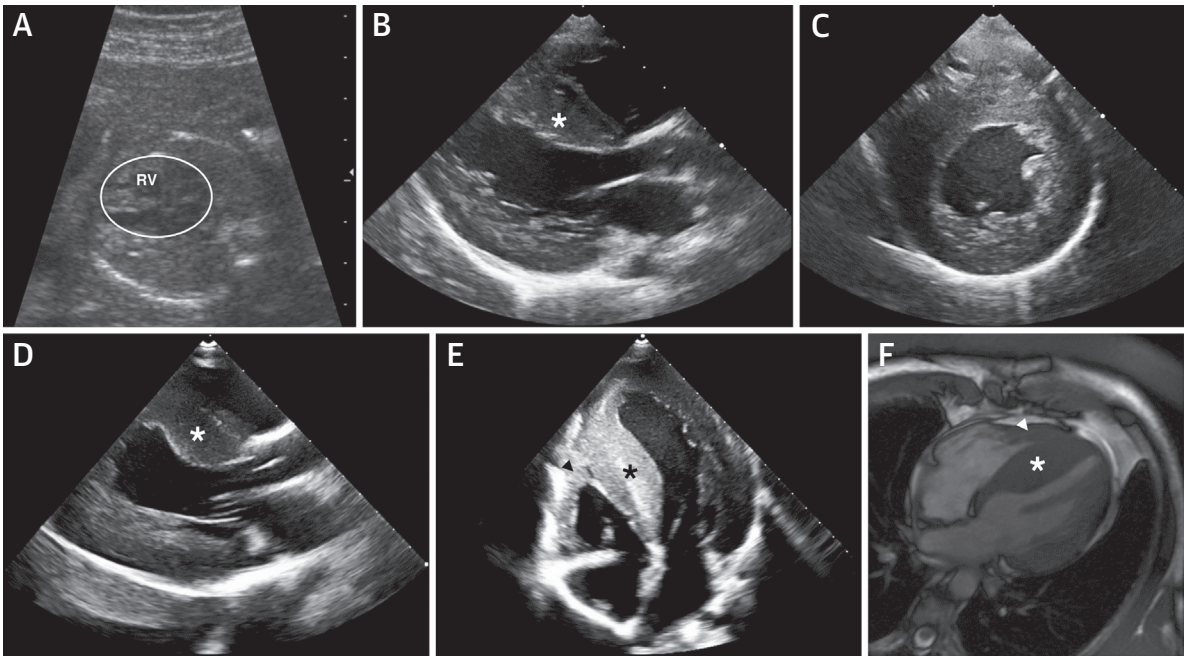

Prenatal ultrasound performed in patient B-IV:2 at 20 weeks of gestation showed an enlarged heart **(encircled)** with right ventricular (RV) hypertrophy **(A)**. Echocardiographic images of the parasternal long-axis **(B)** and short-axis **(C)** views in patient B-IV:3 showed severe concentric left ventricular (LV) hypertrophy. Parasternal long-axis **(D)** and 4-chamber **(E)** views in patient C-V:2 showed severe concentric LV hypertrophy and moderate RV hypertrophy. **(F)** Cardiac magnetic resonance image in patient C-IV:2 showed atypical distribution of LV hypertrophy with relative sparing of the basal segments, and RV hypertrophy. **Asterisks** = interventricular septum; **arrowhead** = RV hypertrophy. Abbreviations as in Figure 1.

developed. The patient was born at 36 weeks (IV:2) (Figure 1B) and presented with severe respiratory distress. Echocardiography revealed severe hypertrophy and dilation of both ventricles. She died 2 h post-partum. Her parents agreed to a detailed post-mortem examination of the heart (discussed in the Histology section later). In the fourth dizygotic twin pregnancy, extensive prenatal ultrasounds revealed no abnormalities. The twin girls were born at 37 weeks. Echocardiography at day 4 showed severe concentric HCM in 1 of the twins (IV:3) (Figure 1B), which remained stable over subsequent years. Cardiac examination in patient IV:3 at age 10 years showed increased thickness of the interventricular septum (IVS) (IVS thickness 13 mm, z-score +6) and LV posterior wall (LVPW) (LVPW thickness 15 mm, z-score +9.5) (Figures 2B and 2C), biventricular diastolic dysfunction, and repolarization abnormalities. There were no ventricular arrhythmias. Family history was negative for sudden cardiac death or cardiomyopathies. Echocardiography revealed no abnormalities in either parent (ages 39 and 22 years) or the twin sister (age 2 months).

For family C, the index patient (C-V:2) was the second child of consanguineous Turkish parents. He was diagnosed with severe HCM at 4 years of age with subsequent slow disease progression. Out-of-hospital cardiac arrest occurred at age 7 years due to ventricular arrhythmias, after which an implantable cardiac-defibrillator (ICD) was placed; he has since experienced several appropriate ICD shocks. Cardiac examination at age 11 years showed severe concentric LV hypertrophy (IVS 20 mm, z-score +11.2; LVPW 19 mm, z-score +13.1) without LV outflow tract obstruction (Figures 2D and 2E), moderate hypertrophy of the right ventricle (RV), and repolarization abnormalities. His father (C-IV:2) was diagnosed with HCM at age 27 years. Cardiac magnetic resonance imaging at age 37 years showed concentric LV hypertrophy, most pronounced in the septum (IVS 32 mm) with relative sparing of the basal segments, and RV hypertrophy (Figure 2F). Echocardiographic screening in the mother (age 42 years) and older brother (age 19 years) revealed no abnormalities. A paternal uncle (C-IV:1) had been diagnosed with HCM at 29 years. Cardiac examination at 45 years of age showed asymmetric septal hypertrophy (IVS 17 mm; LVPW 11 mm) and RV hypertrophy (7 to 8 mm; normal cutoff: 5 mm).

HOMOZYGOSITY MAPPING. In family A, we identified 2 chromosomal regions that were homozygous in the affected boy (IX:2) and heterozygous in his parents (VIII:1 and VIII:2) and unaffected brother (IX:1): 15q25.2q25.3 (84,058,592 to 89,164,874) and 21q21.3q22.11 (29,440,969 to 35,838,907). In family B, we identified 3 homozygous chromosomal regions shared by all affected individuals (IV:1, IV:2, and IV:3), whereas the unaffected father (III:1) and sister (IV:4) were heterozygous: 5q14.3q15 (90,263,863 to 95,782,290), 15q25.1q25.3 (79,333,228 to 87,165,178), and 16q23.2q24.3 (81,602,681 to 90,148,796) (NCBI Build GRCh37/hg19). A small region (3.1 Mb) of homozygosity on chromosome region 15q25 overlapped between the affected individuals from both families.

EXOME VARIANT FILTERING. Exome sequencing was performed to target all exons and exon-intron junction sequences of known genes in the human genome for potential disease-causing variants. Using the filtering pipeline discussed earlier, affected individuals from families A and B were found to harbor a homozygous variant in the *ALPK3* gene (Online Table 2), located in the overlapping region of homozygosity on chromosome 15q25. Patient A-IX:2 was found to carry a homozygous intronic variant in the consensus acceptor splice site sequence of exon 10 of the *ALPK3* gene (c.4736-1G>A) (Figure 3), and this result was validated using Sanger sequencing. Both parents and 2 unaffected siblings (A-IX:1 and IX:3) were heterozygous for the mutation. One unaffected sibling (A-IX:4) carried the normal genotype. Patient B-IV:3 harbored a homozygous variant in exon 6 of the *ALPK3* gene introducing a premature stop codon (c.3781C>T, p.Arg1261*) (Figure 3). Sanger sequencing proved that all affected children were homozygous for this mutation. The father and unaffected sibling (B-IV:4) were heterozygous for the mutation. The mother was unavailable for testing, but is presumed to be a heterozygous carrier of the mutation as well.

***ALPK3* MUTATIONAL SCREENING.** Subsequent Sanger sequencing of all coding regions and flanking intronic sequences of the *ALPK3* gene in a cohort of 60 unrelated patients with childhood-onset HCM or DCM uncovered the homozygous nucleotide substitution c.5294G>A in exon 12 introducing a premature stop codon (p.Trp1765*) in a third patient (family C) (Figure 1C, Table 1). His affected father and paternal uncle were heterozygous carriers; no additional mutation in the known cardiomyopathy genes was found (Online Appendix). In the remaining cohort, no additional mutations in *ALPK3* were identified. Further studies will be performed in these patients to discover novel disease genes.

SPLICE VARIANT ANALYSIS. The c.4736-1G>A variant in intron 9 (family A) was predicted to impair the natural acceptor splice site recognition using in silico tools. Sanger sequencing of cDNA from cultured

FIGURE 3 ***ALPK3*** **Gene Schematic**

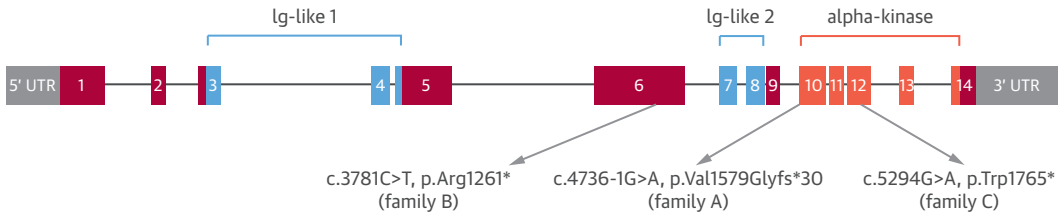

The 3 main functional domains—2 immunoglobulin (Ig)-like domains **(blue)** and 1 alpha-type protein kinase domain **(red)**—and the positions of identified *ALPK3* mutations are indicated. **Boxes** = exons and untranslated regions (UTR); **connecting lines** = intervening introns. Abbreviations as in Figure 1.

fibroblasts of patient A-IX:2 confirmed skipping of exon 10, leading to a deletion of 281 nucleotides (Online Figure 1). At the protein level, a frameshift starting at codon Val1579 and ending in a stop codon 29 position downstream (p.Val1579Glyfs*30) is predicted.

HISTOLOGY. Post-mortem macroscopic examination of the heart of individual A-IX:2 revealed severe cardiomegaly (total weight 34.0 g; normal 13.7 g) and biventricular dilation. Microscopic examination of the myocardium showed subendocardial fibroelastosis without fatty replacement in both ventricles, fragmented elastin fibers, and myxoid degeneration of the stroma (Figure 4A). Post-mortem macroscopic examination of the heart of individual B-IV:2 revealed severe cardiomegaly (total weight 34.7 g; normal

FIGURE 4 **Histopathological Examination of Heart Tissue in** ***ALPK3*****-Related Cardiomyopathy**

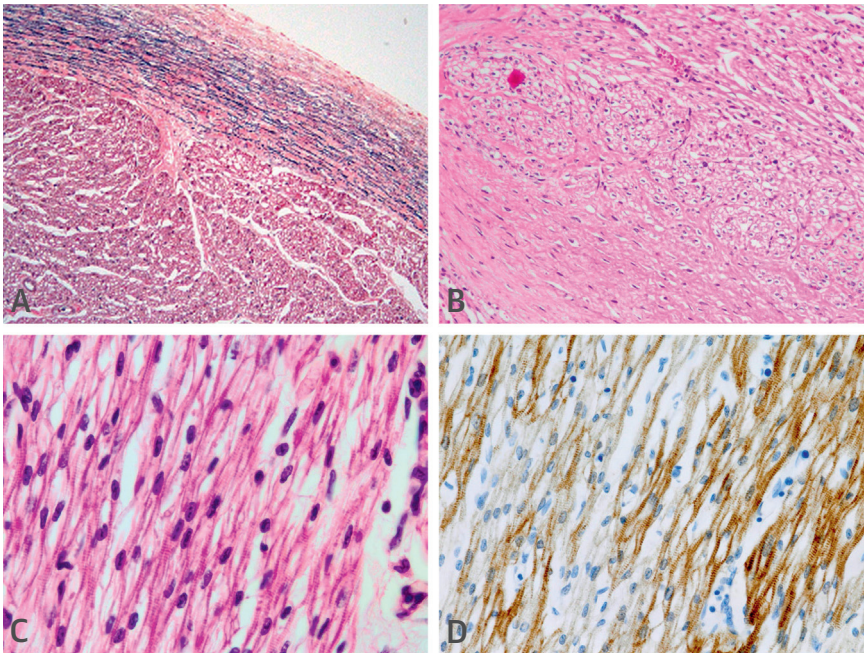

In patient A-IX:2, Verhoeff-van Gieson staining for elastin at 20× magnification showed subendocardial fibroelastosis **(A)**. In patient B-IV:2, hematoxylin and eosin staining at 100× **(B)** and 630× magnification **(C)** showed focal hypertrophy of cardiomyocytes and subendocardial fibroelastosis without fatty infiltration; desmin staining **(D)** showed no apparent myocyte disarray. Intercalated discs were difficult to recognize in patient B-IV:2 and age-matched controls (data not shown). Abbreviations as in Figure 1.

15.5 g) and biventricular dilation with a large adherent thrombus to the left ventricle. Microscopic examination showed focal hypertrophy of the cardiomyocytes and extensive fibroelastosis in the subendocardial region without fatty infiltration (Figures 4B and 4C). No apparent myocyte disarray was observed both on evaluation with hematoxylin and eosin staining, and immunohistochemical staining for desmin (Figure 4D). Intercalated discs were difficult to recognize in both the patients and age-matched controls. Muscle biopsies from individual B-IV:3 (affected) and B-IV:4 (unaffected carrier) did not show any changes at routine histological and enzyme histochemical evaluation, including acid phosphatase, nicotinamide adenine dinucleotide + hydrogen-tetrazolium reductase, succinate dehydrogenase, and cytochrome C oxidase.

IMMUNOHISTOCHEMISTRY. To determine the effects of *ALPK3* mutations at the level of the intercalated discs, we performed immunohistochemical analysis of junctional proteins in cardiac tissue from 1 patient (A-IX:2) and 2 age-matched controls. Immunoreactive signal levels for the desmosomal proteins plakoglobin and desmoplakin were absent at intercalated discs in the patient sample. Signal levels for the other desmosomal protein plakophilin-2, the adhesion molecule N-cadherin, and the gap-junction protein connexin-43 were normal compared with controls (Figure 5). Results of desmin staining were inconclusive (data not shown), as intercalated discs were difficult to recognize in both the patient and control samples.

DISCUSSION

We identified a novel gene, *ALPK3*, involved in human cardiomyopathy (Central Illustration). Biallelic truncating *ALPK3* mutations were identified in 5 patients with diverse ethnic backgrounds who presented with severe, early-onset cardiomyopathy. Four patients were diagnosed during fetal life or within hours of birth. The fifth patient was asymptomatic until the age of 4 years. Three of 5 patients died due to progressive heart failure between 35 weeks of gestation and 5 days after birth. The patients who died exhibited features of DCM or a combination of DCM and HCM. Two patients, who were still alive at age 11 years, showed severe concentric HCM. Although classic HCM and DCM primarily affect the left ventricle, 3 patients also displayed significant RV involvement. Interestingly, 2 heterozygous family

FIGURE 5 Immunofluorescence Images of Myocardial Tissue

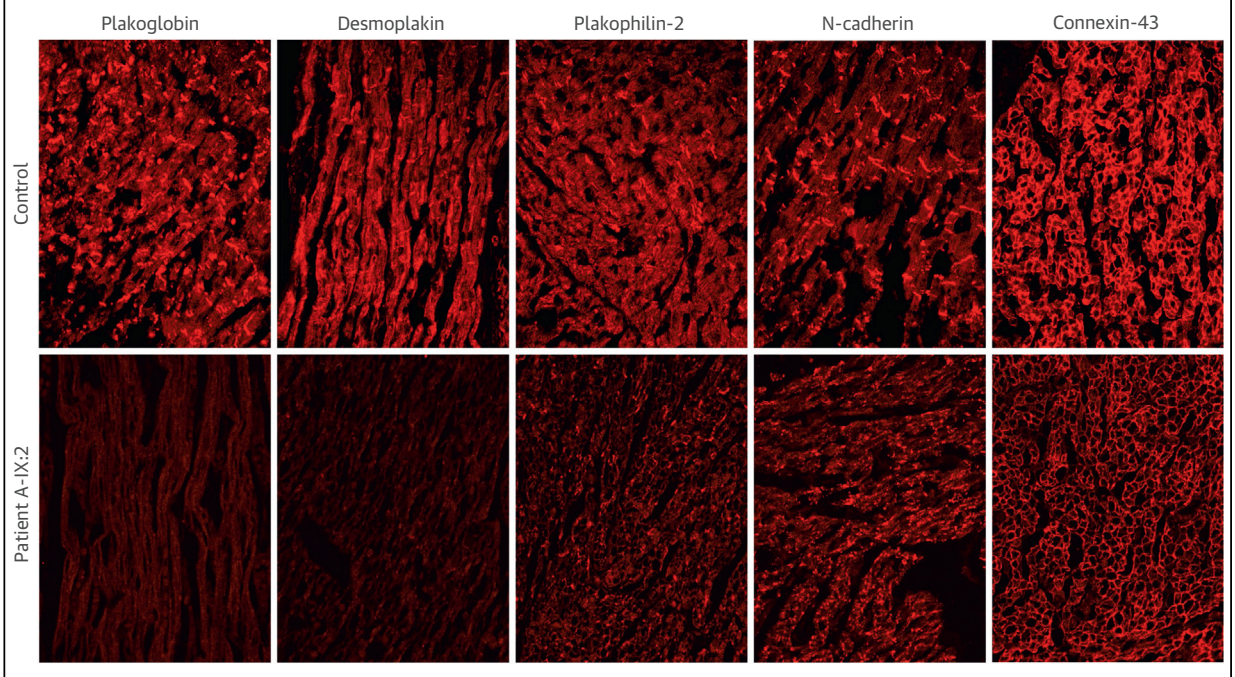

Immunoreactive signals for plakoglobin and desmoplakin are absent at intercalated discs in the sample from patient A-IX:2, whereas signal levels for plakophilin-2, N-cadherin, and connexin-43 are normal when compared with the control samples.

CENTRAL ILLUSTRATION ***ALPK3*-Related Cardiomyopathy: Hypothetical Disease Model**

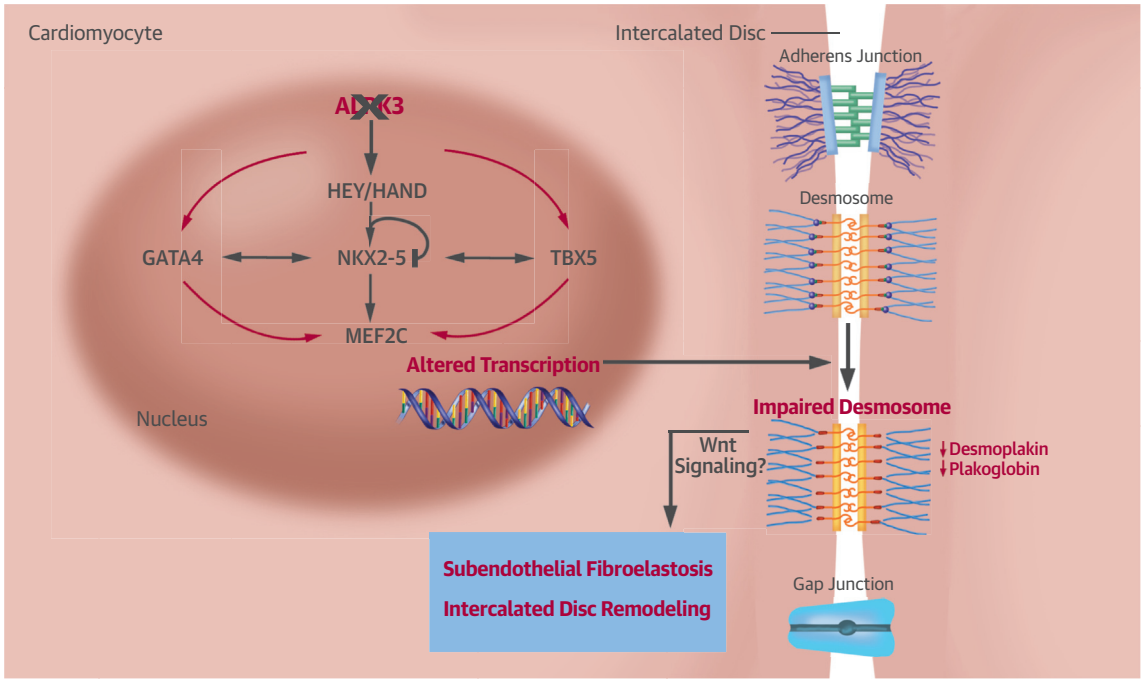

Almomani, R. et al. J Am Coll Cardiol. 2016; 67(5):515–25.

Deficiency of alpha-kinase 3 (ALPK3) modifies the expression of other transcription factors and downstream target genes. These changes affect desmosome composition and will, putatively via modified Wnt signaling, ultimately result in alterations of cellular processes, like subendothelial fibroelastosis and intercalated disc remodeling, characteristic of cardiomyopathy.

members (C-IV:1 and IV:2) were diagnosed with an atypical form of HCM at a young adult age. Cardiac examination of the other proven and obligate heterozygotes (n = 8; age range 2 months to 42 years) revealed no evidence of cardiomyopathy. Although these numbers are limited, one may surmise that *ALPK3* mutation carriers have an increased risk of developing cardiomyopathy; therefore, periodic screening should be considered.

The *ALPK3* gene is the human ortholog of the murine Myocytic induction/differentiation originator (also known as *Midori*). In 2001, the *Alpk3* gene was identified by applying a differential display technique in the P19CL6 cell line, which can be differentiated into beating cardiomyocytes upon incubation with dimethyl sulfoxide. Overexpression of *Alpk3* promoted their differentiation into cardiomyocytes, whereas differentiation was inhibited by blockade of *Alpk3* expression (15). The gene has been mapped to chromosome 15q25.2 and contains 14 exons (**Figure 3**). The ALPK3 protein contains 2 immunoglobulin (Ig)-like domains and an alpha-type protein kinase domain. All 3 private homozygous mutations identified in this study are predicted to create premature stop codons, leading to nonsense-mediated decay or truncated proteins with partial or complete removal of the kinase domain (**Figure 3**). We therefore hypothesize that these mutations result in loss of function of ALPK3. Alpha-kinase 3 belongs to a family of atypical protein kinases that recognize phosphorylation sites in the context of alpha-helices. Alpha-kinases are known to regulate a wide range of cellular processes, including cell migration, adhesion and proliferation, protein translation, vesicular transport, and magnesium homeostasis (16,17).

In mouse embryos, expression of *Alpk3* was restricted to fetal and adult hearts and adult skeletal muscle. Interestingly, *Alpk3* knockout mice display cardiomyopathy with striking similarities to the human phenotype described here (18). Although concentric cardiac hypertrophy of both the left and right ventricle was the predominant feature in *Alpk3*-deficient mice, other changes typically associated with DCM were also observed such as increased

end-diastolic and end-systolic LV volume and a reduction in cardiac outflow, stroke volume, and ejection fraction (18).

Detailed histological and ultrastructural analysis of hearts from *Alpk3*$^{-/-}$ mice showed markedly reduced numbers of indistinct and fragmented intercalated discs and diffuse mild myofibrillar disarray, resulting in looser arrangement of adjacent myofibrils (18). Interstitial fibrosis, 1 of the pathological hallmarks of cardiomyopathies, was absent. In contrast to the observations in *Alpk3* knockout mice, we observed extensive fibroelastosis without apparent myocyte disarray in our human cardiac samples (**Figure 4**).

Intercalated discs play an essential role in the mechanical and electrochemical coupling between adjacent cardiomyocytes. There are 3 main junctional complexes within the disc: fascia adherens, desmosomes, and gap junctions. At an early age, intercalated discs are difficult to visualize under light microscopy, as exemplified in this study. Unfortunately, no patient material was available for ultrastructural examination using electron microscopy. However, immunohistochemical analysis in myocardial tissue from 1 patient revealed the absence of desmosomal proteins plakoglobin and desmoplakin signals at the intercalated discs, whereas signals for the other junctional proteins were normal (**Figure 5**). Reduced immunoreactive signals for plakoglobin at cell-cell junctions have been observed in the majority of patients with arrhythmogenic RV cardiomyopathy. The specificity of this finding, however, remains under debate (14,19). Redistribution of plakoglobin from intercellular junctions to the intracellular space is believed to suppress canonical Wnt/beta-catenin signaling, leading to enhanced fibrogenesis and myocyte apoptosis (20). Reduced signal levels for desmoplakin at intercalated discs, on the other hand, have mainly been demonstrated in patients with end-stage DCM due to mutations in the gene encoding desmin (21). Although our findings support a role for *ALPK3* in the formation and maintenance of intercalated discs, further studies in a larger cohort of patients are needed for validation.

The molecular mechanisms involved in the earliest stages of cardiac development are still largely unknown. *ALPK3* is expressed from the very early stage of cardiogenesis, before key transcription factors, such as the NK-2 class homeobox transcription factor *NKX2-5*, the GATA-binding protein *GATA4*, and the MADS-box transcription enhancer factor *MEF2C* (15). Some cardiac transcription factors (e.g., HEY and HAND proteins) contain a helix-loop-helix domain, characterized by 2 alpha helices separated by a flexible loop structure, and might therefore be targets of *ALPK3*. By regulating the expression of these transcription factors, *ALPK3* might control initial induction of differentiation and maturation of cardiomyocytes. Mutations in these putative downstream targets of *ALPK3* have previously been associated with various congenital heart malformations and arrhythmias in humans (22). Structural heart abnormalities were not observed in the patients described in this study. In recent years, however, some of these genes have also been implicated in familial forms of cardiomyopathy, including *NKX2-5*, *GATA4*, *GATA6*, and the T-box transcription factors *TBX5* and *TBX20* (23–27). Interestingly, mice lacking Xin actin-binding repeat-containing protein 1 (*Xirp1*), a downstream target of *Nkx2-5* and *Mef2c*, display intercalated disc abnormalities and cardiac hypertrophy with conduction defects (28). Further research into the transcription factor pathways involved in heart development and the putative role of *ALPK3* in the related processes will provide more insight into the molecular pathways involved in pediatric cardiomyopathy and may have implications for the development of new therapeutic strategies.

STUDY LIMITATIONS. Although our finding that *ALPK3* is the causal gene in 3 unrelated families of different ethnic backgrounds with pediatric cardiomyopathy underscores its contribution to this severe disease, studies in other and larger cohorts to substantiate our findings are warranted. Further protein studies and electron microscopy examination are needed to fully understand the effects of *ALPK3* mutations and to enhance our understanding of underlying mechanisms leading to the clinical phenotype. For example, immunolabeling with ALPK3 antibodies would give insight into its expression in cardiac tissue. Moreover, identifying interacting partner proteins of ALPK3 will lead to identifying downstream-acting proteins involved in the pathogenesis and remodeling of intercalated discs. Unfortunately, these studies are hampered by the limited availability of cardiac tissues of the patients.

CONCLUSIONS

We have shown that biallelic truncating mutations in *ALPK3* led to severe, early-onset pediatric cardiomyopathy in humans. Carriers may develop cardiomyopathy as adults. *ALPK3*-related cardiomyopathy has morphological features of both HCM and DCM, and is characterized by biventricular involvement and atypical distribution of hypertrophy. Our findings emphasize the essential role of cardiac transcription factor pathways in normal myocardial development. Further studies are necessary to

understand how dysregulation of the transcriptional regulatory network results in cardiomyopathy (**Central Illustration**).

ACKNOWLEDGMENTS The authors thank the families for participating in this study. The authors would like also to thank Kate McIntyre for editing this manuscript, and Tom de Vries Lentsch and René Frowijn for photographic artwork.

REPRINT REQUESTS AND CORRESPONDENCE: Dr. Jan D.H. Jongbloed, Department of Genetics, University of Groningen, University Medical Center Groningen, P.O. Box 30.001, 9700 RB Groningen, the Netherlands. E-mail: j.d.h.jongbloed@umcg.nl.

PERSPECTIVES

COMPETENCY IN MEDICAL KNOWLEDGE: Biallelic mutations in *ALPK3*, a transcriptional regulator involved in early cardiomyocyte differentiation, can cause cardiomyopathy in children.

TRANSLATIONAL OUTLOOK: Further research is needed to describe the molecular and cellular mechanisms responsible for the development of cardiomyopathy in patients with *ALPK3* mutations and explore potential therapeutic strategies that target these processes.

REFERENCES

1. Lipshultz SE, Sleeper LA, Towbin JA, et al. The incidence of pediatric cardiomyopathy in two regions of the United States. N Engl J Med 2003;348:1647–55.

2. Daubeney PE, Nugent AW, Chondros P, et al. Clinical features and outcomes of childhood dilated cardiomyopathy: results from a national population-based study. Circulation 2006;114:2671–8.

3. Towbin JA, Lowe AM, Colan SD, et al. Incidence, causes, and outcomes of dilated cardiomyopathy in children. JAMA 2006;296:1867–76.

4. Elliott P, Andersson B, Arbustini E, et al. Classification of the cardiomyopathies: a position statement from the European Society Of Cardiology Working Group on Myocardial and Pericardial Diseases. Eur Heart J 2008;29:270–6.

5. Kindel SJ, Miller EM, Gupta R, et al. Pediatric cardiomyopathy: importance of genetic and metabolic evaluation. J Card Fail 2012;18:396–403.

6. Tariq M, Ware SM. Importance of genetic evaluation and testing in pediatric cardiomyopathy. World J Cardiol 2014;6:1156–65.

7. Seelow D, Schuelke M. HomozygosityMapper2012—bridging the gap between homozygosity mapping and deep sequencing. Nucleic Acids Res 2012;40:W516–20.

8. Boomsma DI, Wijmenga C, Slagboom EP, et al. The Genome of the Netherlands: design, and project goals. Eur J Hum Genet 2014;22:221–7.

9. 1000 Genomes Project Consortium, Abecasis GR, Auton A, Brooks LD, et al. An integrated map of genetic variation from 1,092 human genomes. Nature 2012;491:56–65.

10. den Dunnen JT, Antonarakis SE. Mutation nomenclature extensions and suggestions to describe complex mutations: a discussion. Hum Mutat 2000;15:7–12.

11. Ng PC, Henikoff S. Predicting deleterious amino acid substitutions. Genome Res 2001;11:863–74.

12. Adzhubei IA, Schmidt S, Peshkin L, et al. A method and server for predicting damaging missense mutations. Nat Methods 2010;7:248–9.

13. Schwarz JM, Cooper DN, Schuelke M, Seelow D. MutationTaster2: mutation prediction for the deep-sequencing age. Nat Methods 2014;11:361–2.

14. Asimaki A, Tandri H, Huang H, et al. A new diagnostic test for arrhythmogenic right ventricular cardiomyopathy. N Engl J Med 2009;360:1075–84.

15. Hosoda T, Monzen K, Hiroi Y, et al. A novel myocyte-specific gene Midori promotes the differentiation of P19CL6 cells into cardiomyocytes. J Biol Chem 2001;276:35978–89.

16. Middelbeek J, Clark K, Venselaar H, Huynen MA, van Leeuwen FN. The alpha-kinase family: an exceptional branch on the protein kinase tree. Cell Mol Life Sci 2010;67:875–90.

17. Drennan D, Ryazanov AG. Alpha-kinases: analysis of the family and comparison with conventional protein kinases. Prog Biophys Mol Biol 2004;85:1–32.

18. Van Sligtenhorst I, Ding ZM, Shi ZZ, Read RW, Hansen G, Vogel P. Cardiomyopathy in alpha-kinase 3 (ALPK3)-deficient mice. Vet Pathol 2012;49:131–41.

19. Munkholm J, Christensen AH, Svendsen JH, Andersen CB. Usefulness of immunostaining for plakoglobin as a diagnostic marker of arrhythmogenic right ventricular cardiomyopathy. Am J Cardiol 2012;109:272–5.

20. Garcia-Gras E, Lombardi R, Giocondo MJ, et al. Suppression of canonical Wnt/beta-catenin signaling by nuclear plakoglobin recapitulates phenotype of arrhythmogenic right ventricular cardiomyopathy. J Clin Invest 2006;116:2012–21.

21. Otten E, Asimaki A, Maass A, et al. Desmin mutations as a cause of right ventricular heart failure affect the intercalated disks. Heart Rhythm 2010;7:1058–64.

22. McCulley DJ, Black BL. Transcription factor pathways and congenital heart disease. Curr Top Dev Biol 2012;100:253–77.

23. Pashmforoush M, Lu JT, Chen H, et al. Nkx2-5 pathways and congenital heart disease; loss of ventricular myocyte lineage specification leads to progressive cardiomyopathy and complete heart block. Cell 2004;117:373–86.

24. Li RG, Li L, Qiu XB, et al. GATA4 loss-of-function mutation underlies familial dilated cardiomyopathy. Biochem Biophys Res Commun 2013;439:591–6.

25. Xu L, Zhao L, Yuan F, et al. GATA6 loss-of-function mutations contribute to familial dilated cardiomyopathy. Int J Mol Med 2014;34:1315–22.

26. Zhang XL, Qiu XB, Yuan F, et al. TBX5 loss-of-function mutation contributes to familial dilated cardiomyopathy. Biochem Biophys Res Commun 2015;459:166–71.

27. Kirk EP, Sunde M, Costa MW, et al. Mutations in cardiac T-box factor gene TBX20 are associated with diverse cardiac pathologies, including defects of septation and valvulogenesis and cardiomyopathy. Am J Hum Genet 2007;81:280–91.

28. Gustafson-Wagner EA, Sinn HW, Chen YL, et al. Loss of mXinalpha, an intercalated disk protein, results in cardiac hypertrophy and cardiomyopathy with conduction defects. Am J Physiol Heart Circ Physiol 2007;293:H2680–92.

KEY WORDS exome sequencing, homozygous alpha-kinase 3 mutations, hypertrophy, intercalated disc

APPENDIX For an expanded Methods section as well as supplemental tables and a figure, please see the online version of this article.